

Accepted Manuscript

Absence of mitochondrial uncoupling protein 3: Effect on thymus and spleen in the fed and fasted mice

Orlagh M. Kelly, Richard K. Porter

PII: S0005-2728(11)00143-5
DOI: doi: [10.1016/j.bbabbio.2011.06.002](https://doi.org/10.1016/j.bbabbio.2011.06.002)
Reference: BBABIO 46722

To appear in: *BBA - Bioenergetics*

Received date: 4 March 2011
Revised date: 4 June 2011
Accepted date: 6 June 2011



Please cite this article as: Orlagh M. Kelly, Richard K. Porter, Absence of mitochondrial uncoupling protein 3: Effect on thymus and spleen in the fed and fasted mice, *BBA - Bioenergetics* (2011), doi: [10.1016/j.bbabbio.2011.06.002](https://doi.org/10.1016/j.bbabbio.2011.06.002)

This is a PDF file of an unedited manuscript that has been accepted for publication. As a service to our customers we are providing this early version of the manuscript. The manuscript will undergo copyediting, typesetting, and review of the resulting proof before it is published in its final form. Please note that during the production process errors may be discovered which could affect the content, and all legal disclaimers that apply to the journal pertain.

Absence of mitochondrial uncoupling protein 3: Effect on thymus and spleen in
the fed and fasted mice.

Orlagh M. Kelly and Richard K. Porter

School of Biochemistry and Immunology, Trinity College Dublin, Dublin 2, Ireland

*Corresponding Author: Richard K. Porter, Tel: +353-1-8961617; Fax: +353-1-6772400; e-mail:
rkporter@tcd.ie*

Abbreviations: BCA, bichinchonic acid; BSA, bovine serum albumin; DP, CD4⁺/CD8⁺ double positive; DN, CD4⁻/CD8⁻ double negative; DEX, dexamethasone; ECL, enhanced chemiluminescence; EGTA, ethylene glycol-bis(2-aminoethylether)-*N,N,N',N'*-tetraacetic acid; FBS, fetal bovine serum; FCCP, carbonylcyanide-4-(trifluoromethoxy)-phenylhydrazone; FITC, fluorescein isothiocyanate; PBS, phosphate buffered saline; SP, single positive; PI, propidium iodide; PDH, pyruvate dehydrogenase; PVDF, polyvinylidene difluoride; R-PE, R-phycoerythrin; RPMI, Roswell Park Memorial Institute; TBS, tris buffered saline; UCP, uncoupling protein; WT, wild-type

Abstract

Mitochondrial uncoupling protein 3 (UCP3) is constitutively expressed in mitochondria from thymus and spleen of mice, and confocal microscopy has been used to visualize UCP3 in situ in mouse thymocytes. UCP3 is present decrease by a half in thymus and a fifth in spleen after three weeks, probably reflecting the suckling to weaning transition. UCP3 protein levels increase ~3-fold in thymus on starvation, but expression levels in spleen were unaffected by starvation. Lack of UCP3 had little effect on thymus mass or thymocyte number. However, lack of UCP3 affected spleen mass and splenocyte number (in the fasted state) and results in reduced CD4⁺ single positive cell numbers and reduced double negative cells in the thymus, but as a 2-fold increase in the proportion of CD4⁺, CD8⁺ and DP cells in spleen. Starvation attenuates these proportionate differences in the spleen. A lack of UCP3 had no apparent effect on basal oxygen consumption of thymocytes or splenocytes or on oxygen consumption due to mitochondrial proton leak. Splenocytes from UCP3 knock-out mice are also more resistant to apoptosis than those from wild-type mice. Overall we can conclude that UCP3 affects thymocyte and spleen cell profiles in the fed and fasted state.

Research Highlights

This is the first study to definitively demonstrate the presence of mitochondrial uncoupling protein 3 (UCP3) in thymocytes and splenocytes and we provide evidence that UCP3 plays a role in thymocyte and spleen cell selection in the fed and fasted state.

1. INTRODUCTION

UCP3 is predominantly found associated with skeletal muscle mitochondria [1-3], however it is still not clear what UCP3 actually catalyzes in vivo. One constant is the physiological observation that increased UCP3 protein expression levels are associated with conditions where fatty acid oxidation is increased e.g. conditions such as starvation and hyperthyroidism [2,4-7]. Several studies on isolated skeletal muscle mitochondria suggest that UCP3 is an uncoupler of oxidative phosphorylation either by being a catalyst for fatty acid oxidation products from the mitochondrial matrix [8] or by being activated to catalyse a proton leak by fatty acid oxidation products such as 4-hydroxy-2-nonenal [9,10], although the specificity of the latter has been challenged [11]. Interestingly, sequence analysis and (pseudo)symmetry modelling based on known mitochondrial transporters, predict that UCP's are keto-acid transporters [12]. UCP3 protein has also been detected in highly metabolic tissues such as brown fat tissue [13,14] and heart [15], and in skeletal muscle under conditions of high fat diet [16]. However, data from UCP3 knock-out mice show no obvious metabolic phenotype compared to wild-types [17,18].

Interestingly, UCP1, UCP2 and UCP3 protein are found in various immune cells. UCP1 is present in thymocytes and lack of UCP1 has been shown to affect T-lymphocyte selection [19-22]. UCP2 is predominantly found associated with macrophages and the innate immune system, with UCP2 deficient mice, for instance, being proinflammatory and resistant to infection by *Toxoplasma gondii* [23-25], while lack of UCP2 has minimal effect on thymocyte profile [26]. UCP3 has been detected in mitochondria from rat thymus and rat spleen [14] and in this study we investigate the role of UCP3 in thymocyte and T-lymphocyte selection.

The thymus is the site of thymocyte maturation and selection resulting in naïve T-cells which migrate to peripheral lymphoid tissue, such as spleen (for reviews see [26-28]). Thymocytes in the thymus are at different stages of maturation. The most immature of these cells are easily identified due to the lack of the CD4/CD8 surface antigens (CD4/CD8 double negatives DN)) and account for up to ~5% of the cells present in the thymus. Maturation manifests itself as expression of both CD4 and CD8 antigens of the thymocyte surface (CD4/CD8 double positives (DP)), which account for up to 85% of cells in the thymus. The DP cells undergo positive selection for antigen and negative selection for self-antigen resulting in death of up to 95%

of these cells through apoptosis. The remaining DP cells mature to either naïve CD4 single positive (CD4 SP) or naïve CD8 single positive (CD8 SP) cells which enter the medulla of the thymus before migrating to the peripheral immune tissues. In the spleen, CD4 SP T-lymphocytes account for approximately 20% of all cells whereas CD8 SP T-lymphocytes account for approximately 10% of all cells. The remainder of the cells in the spleen are composed mainly of reticulocytes, monocytes and B-lymphocytes with a negligible number of CD4/CD8 DP T-lymphocytes [29,30]. In this study we investigated whether there was UCP3 expression in thymus and spleen of mice, whether lack of UCP3 in thymus and spleen results in a difference in thymus and spleen cell composition profile and function when compared to wild-type mice of the same background, sex, age and strain.

2. Material and Methods

2.1 Reagents

All reagents and chemicals used were of analytical grade where possible and were obtained from Sigma Chemical Co. Ltd, Fancy Rd., Poole, Dorset, U.K. unless otherwise stated.

2.2 Animal Source

UCP3 ^{-/-} mice on a 129 background, originally provided by Prof. Padraic Fallon (Institute of Molecular Medicine, Trinity College Health Sciences Centre, St James' Hospital, Dublin) were bred in-house. Animals were housed in a specific pathogen free environment. Wild-Type 129 mice and UCP3^{-/-} were housed at 25±1°C. All animals were allowed free access to food (except those on a 24h starvation regime) and water and a 12-hour light/dark cycle was in place. All mice were killed by CO₂ asphyxiation.

2.3 Cell isolation

Thymocytes were isolated from UCP3 ^{-/-} and wild type mice essentially as described by Buttgerit and Brand [31]. The thymus was removed, trimmed clean of connective tissue and brown fat (if present) and transferred into Hanks' Balanced Salt Solution (Sigma) containing 10% (w/v) foetal bovine serum (FBS). A single cell suspension was prepared by passage through a 70µm nylon sieve (Falcon).

Spleen cells were isolated according to the method of Mills et al. [29]. The spleen was removed from the abdominal cavity, trimmed free of connective tissue and transferred to RPMI-1640 medium containing L-glutamine. The spleen and medium was poured onto a 70µm nylon sieve (Falcon) in a Petri dish and, using a plunger of a 5ml syringe, the spleen was ground until a fine suspension of spleen cells were obtained. This suspension of splenocytes was transferred to a 15ml centrifuge tube, using a Pasteur pipette, and allowed to stand for 10 min at room temperature to ensure that debris and cell clumps settle to the bottom of the centrifuge tube. The splenocytes in the supernatant were aspirated off and transferred to a fresh 15ml centrifuge tube. The splenocytes were centrifuged at 300g for 5 min in a bench-top centrifuge. The cell pellet was re-suspended in RPMI-1640.

Cells were counted using the Trypan Blue exclusion method. 0.05 ml of 0.1% (w/v) trypan blue, 0.03 ml RPMI-1640 (10% FBS and L-glutamine) and 0.02 ml of cell suspension were added together and left at room temperature for 10 minutes prior to counting. Cell count was performed using a haemocytometer.

2.4- Isolation of mitochondria from thymus and spleen

Mitochondria were isolated from thymus and spleen tissues by differential centrifugation essentially as described by Chappell and Hansford [32]. Thymus or spleen tissues were suspended in ice-cold (0-4°C) buffer (250mM Sucrose, 5mM Trizma-base, 2mM EGTA, pH 7.4). The cell suspensions were poured into a 2ml Potter homogeniser tube to a final volume of about 1.5ml. The tissue suspensions were then homogenised by hand, with 6 passes using a pestle of 0.12 inch (tight) clearance. The homogenates were centrifuged at 800g for 3 min at 4°C. The pellets were discarded and the supernatants were centrifuged at 12,000g for 10 min at 4°C yielding a "mitochondrial" pellet. The supernatants were discarded and the pellets were resuspended in buffer and re-centrifuged at 12,000g for 10 min at 4°C. The pellets were resuspended in

buffer and re-centrifuged as above. The resulting pellets, containing the mitochondrial fraction, were resuspended in buffer to the desired concentration and stored on ice prior to analysis.

2.5. Indirect Immunofluorescence

Isolated thymocytes were prepared for indirect immunofluorescence essentially as described in Adams et al. [22]. Thymocytes were suspended in Hanks medium (and 10% FBS). 0.5% (v/v) paraformaldehyde was added to 1ml of thymocytes and incubated on ice for 5 minutes. 20 μ l of cells were added to the slides (poly-*l*-lysine coated) and allowed to dry (phosphate crystals form). Slides were then dipped in (-20°C) methanol at -20°C for 5min. Slides were then dipped in (-20°C) acetone at -20°C for 5min. Slides were then allowed to dry at room temperature.

The cells on the cover-slips were then incubated with blocking buffer (PBS containing 5% (w/v) BSA and methylamine, 0.1M) for 2h at room temperature in petri dishes, to inactivate any remaining formaldehyde and block non specific binding. The cells on the cover-slips were incubated with primary antibody diluted in PBS containing 5% (w/v) BSA overnight at room temperature. Following washing with PBS the cells on the cover-slips were incubated with the secondary antibody conjugated to a fluor diluted with PBS for 3h at room temperature. The cells on the cover-slips were then washed with PBS (and sodium azide) and finally mounted onto glass slides using 5 μ l of anti-quench solution.

2.6 Preparation of anti-quench

The anti-oxidant *n*-propyl gallate (4%, v/v) was dissolved in PBS buffer containing sodium azide (15mM) and glycerol (50%, w/v). 0.1 μ g/ml Hoeschst stain was also added. This solution was always made fresh on the day and stored at 4°C in the dark until required.

2.7- Confocal microscopy

Confocal microscopy was performed essentially as described by Adams et al. [21,22]. The 12 well plates with anti-quench solution were covered with cover-slips and were affixed to the glass slide by applying a thin film of nail varnish to the edges of the cover-slip. This procedure also prevented the samples from drying out. The slides were examined by phase contrast and confocal microscopy with an Olympus Fluoview FV1000 Imaging system. The excitation light for imaging was provided by the 457-514 nm lines of a multi-line Argon laser, the 543nm line of a Green Helium - Neon laser and the 633 nm line of a red helium-Neon laser. Images were collected and processed with the Olympus Fluoview software (version 1.3c). Thymocytes were probed with FITC-conjugated anti-Thy1 antibody (BD Biosciences, green) and UCP3 antibody (custom made by Eurogentec) using an Alexa 647 labelled secondary antibody (Invitrogen-red)

2.8 Flow Cytometry- Cell detection

Thymocytes/splenocytes were washed and adjusted to 5×10^6 /ml in PBSA (1% (w/v) BSA-PBS) and 50 μ l was used for each sample. Cells were incubated on ice for 15min in the dark with the surface staining antibodies (CD4-FITC and CD8-R-PE). Fixation medium (Caltag A; Invitrogen) was added to each tube, followed by incubation on ice for 15mins. Cells were washed twice in PBSA and 30 000 events collected on a DakoCyan ADP flow cytometer. Data was analysed using Flowjo software.

2.9 Thymocyte incubations with dexamethasone

Thymocytes were isolated as previously described [31]. Thymocytes were seeded in RPMI-1640 medium supplemented with 10% (w/v) heat-inactivated fetal bovine serum, 2 μ M L-glutamine, penicillin (100U/ml) and streptomycin (100 μ g/ml) in the presence or absence (just vehicle, ethanol) of 0.1 μ M dexamethasone for up to six hours in a 37°C humidified incubator under an atmosphere of 5% (v/v) CO₂.

2.10 Mitochondrial protein determination using the bicinchoninic acid assay

Quantification of protein concentrations in mitochondrial samples was carried out using the bicinchoninic acid assay described by Smith et al. [33]. This measures the formation of Cu⁺ from Cu²⁺ by the Biuret

complex in alkaline solutions of protein. All of the following solutions (standards or samples) were directly prepared in a 96-well plate. A standard protein solution of BSA was suitably diluted in deionised water from 0 to 0.25mg.ml⁻¹. The amount of mitochondrial protein present in the samples was determined by reference to a standard curve derived from the above known concentrations of BSA. Isolated mitochondria were diluted in H₂O before analysis to ensure the final concentration of the samples would fall within the range of the standard curve. Once the samples and the standards were prepared, 200µl of a working solution of BCA (1:49 (v/v) BCA: Cu₂SO₄) was added to each well. The plate was then incubated for 30 minutes in an incubator set at 37°C. The absorbance of each sample was measured spectrophotometrically at 550nm.

2.11 SDS-PAGE and Western Blot analysis:

One-dimensional SDS-PAGE under reducing conditions was used to separate proteins prior to immunoblot analysis, as described by Cunningham et al. [2]. Following SDS-PAGE, resolved proteins were transferred onto polyvinylidene difluoride (PVDF) membranes (Immobilin-P^{SO}; Millipore) as described by Cunningham et al. [2]. the anti-UCP3 polypeptide antibody (amino acids 141-156) was custom made by Eurogentec as previously reported. The pyruvate dehydrogenase (PDH) E₁α monoclonal antibody was from MitoSciences. The primary antibodies were all used at 1:1000 dilution. Following blocking and overnight primary antibody incubation, the blots were incubated with a horseradish peroxidase-conjugated goat anti-rabbit secondary antibody (1:10,000) in Tris-buffered saline (TBS), 0.5% (v/v) Tween 20, 5% (w/v) bovine serum albumin for 1h at room temperature. Blots were developed using an ECL detection system (Amersham Biosciences), and immunoreactions were visualized by exposure to Kodak X-Omat LS film.

2.12 Densitometry

Following immunoblot analysis, the relative abundance to protein was determined using densitometry. The band intensities of the exposed film were analysed using Scion Imaging Software.

2.13- Thymocyte/splenocyte induction of apoptosis

Thymocytes/splenocytes were seeded in RPMI-1640 medium supplemented with 10% (w/v) heat-inactivated fetal bovine serum, 2 μ M L-glutamine, penicillin (100U/ml) and streptomycin (μ g/ml) either in the presence of 0.1 μ M dexamethasone dissolved in ethanol or ethanol alone (vehicle) for up to 20h in a 37°C humidified incubator under an atmosphere of 5% (v/v) CO₂.

2.14 Flow Cytometry FITC-Annexin V /Propidium Iodide (PI) Staining

The apoptotic potential of isolated thymocytes treated with vehicle or dexamethasone was measured as follows: To determine early membrane and DNA changes, whole thymocytes were stained with FITC-conjugated Annexin V and propidium iodide (PI) according to manufacturer's instructions (Molecular Probes). Cells (0.75×10^6) were suspended in 100 μ l of annexin-binding buffer, and 5 μ l of FITC-annexin V and 1 μ l of PI (100 μ g/ml) was added to each 100 μ l cell suspension. Cells were incubated for 15 min at room temperature. Stained cells were suspended in 400 μ l of binding buffer and immediately processed by flow cytometry.

2.15 Measurement of oxygen consumption rates of cells

All measurements of oxygen consumption rate were made using an Oxygraph-2k respirometer (Oroboros Instruments, Innsbrück, Austria), and oxygen flux was resolved using DATLAB software. The oxygraph-2k is a two chamber titration- injection respirometer with a limit of oxygen flux detection of 1pmol/ml⁻¹. Standardized instrumental and chemical calibrations were performed to correct for back diffusion of oxygen into the chamber from the various components; leak from the exterior, oxygen consumption by the chemical medium, and sensor oxygen consumption. The cell suspension was stirred using a PDVF magnetic stirrer and thermostatically maintained at 28°C. Before each experiment medium was equilibrated for 30-40 min with air in the oxygraph chambers until a stable signal was achieved to calibrate for oxygen saturation. Quiescent cell steady state oxygen consumption rates (basal) were then measured in RPMI medium (5×10^6 cells/ml). Subsequent additions included sufficient oligomycin (60ng/ml) to inhibit in situ mitochondrial ATPsynthase and reflect the oxygen due to the proton leak of the in situ mitochondria (Leak) and the mitochondrial uncoupler carbonylcyanide-4-(trifluoromethoxy)-phenylhydrazone (100nM FCCP) was added

to determine the maximal electron chain activity of the in situ mitochondria, as described in Buttgerit and Brand [31]. ATP levels in thymocytes from WT and UCP3 ko mice were measured from a single experiment in triplicate as per Adams et al. [22] but no difference in ATP levels were detected (results not shown).

2.16 Statistical analysis

All results are expressed as mean \pm sem of 'n' determination performed in at least triplicate unless otherwise indicated. Mean values were compared using an unpaired student t-test test. Unless otherwise stated a *p* value of ≤ 0.05 was taken to indicate significance.

3. RESULTS

Figure 1 shows the selectivity of the peptide antibody raised to UCP3. The UCP3 antibody detects UCP3 in both lysates from yeast over-expression UCP3 (Figs. 1A and 1C) and mitochondria isolated from thymus (Fig. 1A) and spleen (Fig. 1C) of wild-type mice. No UCP3 was detected in UCP3 knockout mice or in mouse liver mitochondria, as expected (Figs. 1A and 1C). The presence of mitochondria was confirmed using an antibody to pyruvate dehydrogenase subunit E1 α (Figs. 1B and 1D). These data are consistent with selectivity and sensitivity determinations using this antibody previously reported by Cunningham et al. [2].

We have previously used confocal images of thymocytes to demonstrate expression of UCP1 [21,22]. Here we have used confocal microscopy to demonstrate constitutive UCP3 expression in thymocytes. Figure 2 shows a comparison of thymocytes from wild-type and UCP3^{-/-} mice. The images show (a) localisation of the nucleus within thymocytes from wild-type and UCP3^{-/-} mice using Hoechst stain (b) the labelled surface marker Thy 1 (green) used to identify thymocytes from wild-type and UCP3^{-/-} mice, (c) that UCP3 is present in thymocytes from wild-type mice but absent in thymocytes isolated from UCP3^{-/-} mice, as detected using the peptide antibody shown to be specific for UCP3 and a secondary antibody conjugated to Alexa 647 (red) and (d) phase contrast images of thymocytes from wild-type and UCP3^{-/-} mice.

Figure 3 shows the time-dependent profile of UCP3 expression in mitochondria isolated from thymus and spleen of wild-type mice aged 1, 2, 3, 4, 6, 8 and 16 weeks. Figures 3A and 3D are immunoblots showing the anti-UCP3 peptide antibody detecting UCP3 protein in thymus and spleen mitochondria, but not liver mitochondria (as expected), from mice of different ages. Figure 3B and 3E show that any variance in the expression of UCP3, due to age, cannot be due to differences in lane loading, as indicated by immunoblot with the antibody to PDH-E1- α . Figures 3C and 3F show the collated data, from immunoblots, for thymus and spleen mitochondria, respectively, and the relative abundance of UCP3 protein expression, relative to PDH for 3 separate experiments. A significant reduction in UCP3 expression occurs after 3 weeks and persists in mitochondria from thymus ($p=0.0024$). A significant increase in UCP3 in spleen mitochondria expression occurs between weeks 1 and 3 ($p=0.02$, $n=3$) and between weeks 2 and 3 ($p=0.03$, $n=3$). A significant reduction in UCP3 expression occurs between weeks 3 and 4 ($p=0.02$, $n=3$) and persists from then on.

Figure 4 shows that following 24-hour fasting, UCP3 protein expression is increased in mitochondria isolated from the thymus, but not spleen mitochondria of 129 wild-type mice when compared to fed controls. The UCP3 peptide antibody detects UCP3, in mitochondria of thymus (Fig. 4A) and spleen (Fig. 4D), in lysates of yeast over-expressing UCP3, but not in liver mitochondria, as expected. Figures 3B and 3E show that any variance in the expression of UCP3 cannot be due to differences in lane loading, as indicated by an antibody to PDH-E1- α (Mitosciences). Figures 4C and 4F show the collated immunoblot data for thymus and spleen mitochondria, respectively, as determined by densitometry, and the relative abundance of UCP3 protein expression as a ratio to PDH for 3 separate experiments. There is a significant ($p=0.001$) increase (~3-fold) in UCP3 expression in thymus mitochondria isolated from starved animals compared to fed controls. There is no significant difference in UCP3 expression in spleen mitochondria isolated from starved animals compared to fed controls.

Figure 5 illustrates that there is no significant difference in thymus weight in a comparison of thymuses from wild-type and UCP3 knock-out mice either in the fed or fasted state (Fig. 5A). However there is a significant

reduction ($p=0.016$) in thymus mass due to 24h starvation of wild-type fed mice compared to wild-type fasted animals (Fig. 5A). There is also a significant reduction in the thymus mass of starved UCP3 knock-out mice compared to fed UCP3 knock-out mice ($p=0.009$) (Fig. 5A). Figure 5 also demonstrates that there is no significant difference between the total cell count in the thymus of wild-type mice compared to UCP3 mice in the fed or fasted state (Fig. 5C). However 24h starvation caused a significant reduction ($p=0.038$) in total thymus cell number in wild-type mice (Fig. 5C), and in UCP3 knock-out mice (Fig. 5C)($p=0.02$).

Figure 5 also illustrates that there is no significant difference in spleen mass in a comparison of spleens from wild-type and UCP3 knock-out mice in the fed state (Fig. 5B). However, there is a significant ($p=0.002$) 1.25-fold reduction in spleen mass in the absence of UCP3 in the fasted state (Fig. 5B). 24h starvation had no significant effect on spleen mass of wild-type fed mice compared to wild-type fasted animals (Fig. 5B) or in the spleen mass of starved UCP3 knock-out mice compared to fed UCP3 knock-out mice (Fig. 5B). We also observed no significant difference between the total cell count in the spleen of wild-type mice compared to UCP3 knock-out mice in the fed state (Fig. 5D). However there is a significant ($p=0.004$) 1.25-fold reduction in the number of splenocytes in the fasted state (Fig. 5D) of wild-type mice compared to UCP3 knockout mice. Furthermore, 24h starvation caused a significant reduction ($p=0.05$) in total spleen cell number in wild-type mice (Fig. 5D), and in UCP3 knock-out mice (Fig. 5D)($p=0.004$).

Figure 6A and 6B demonstrates a comparison of oxygen consumption rates by thymocytes and splenocytes isolated from wild-type and UCP3 knock-out mice. Rates were measured for quiescent cells (basal), cells that were treated with oligomycin, thus inhibiting the mitochondrial ATP synthase, resulting in reduced oxygen consumption rates predominantly due to proton leak (leak) and in the presence of a mitochondrial uncoupler, thus giving maximal mitochondrial oxygen consumption (FCCP). Interestingly, no significant differences were observed in the aforementioned comparisons. Furthermore, starvation had no significant effect on the in these vitro oxygen consumptions rates for the aforementioned comparisons (Fig. 6C and 6D).

Figure 7A-F displays the proportion of thymocytes that are CD4 single positive (CD4SP), CD8 single positive (CD8SP), CD4CD8 double negative (DN) and CD4CD8 double positive (DP) in a comparison of wild-type and UCP3 knock-out (UCP3^{-/-}) mice in the fed state. The data demonstrates that there is a significant (2.5-fold, $p=0.0001$) reduction in the abundance of CD4 single positive (Fig. 7A) and a significant (1.4-fold, $p=0.0001$) reduction in CD4CD8 double negative cells (Fig. 7E) in the thymuses of UCP3 knock-out mice compared to that of wild-type controls. No significant reduction in CD8SP (Fig. 7D) or DP cell (Fig. 7F) subsets were observed in thymuses from UCP3 knock and wild-type mice. Representative dot-plots for thymocytes from fed wild-type and UCP3 ^{-/-} are shown (Fig. 7A and 7B). Figure 7G-L displays the proportion of thymocytes that are CD4SP, CD8SP, DN and DP in a comparison of wild-type and UCP3 knock-out mice in the fasted state. The data demonstrates that there is a significant (1.25-fold, $p=0.007$) reduction in the abundance of CD4 SP (Fig. 7I), and a significant decrease in the CD8SP cell number (Fig. 7J) (1.3-fold, $p=0.0005$) in the thymuses of UCP3 knock-out mice compared to that of wild-type controls. No significant reduction in DN (Fig. 7K) or DP cell subsets were observed in thymuses from UCP3 knock-out and wild-type mice, if anything there was a slight increase in DP in UCP3 knock-out mice compared to wild-type controls (Fig. 7L). Representative dot-plots for thymocytes from fasted wild-type and UCP3 ^{-/-} are shown (Fig. 7G and 7H).

Comparing the data from the fed and fasted states and whether there is any effect on the relative proportion of thymocyte subsets from UCP3 knock-out and wild type mice it would appear that starvation attenuates differences in the abundance of CD4SP (Fig. 7C and 7I) and DN (Fig. 7E and 7K). Starvation has no effect on the proportions of DP cell (Fig. 7F and 7L), but result in a significant ($p=0.0005$) 1.3-fold reduction in the proportion CD8SP cells (Fig. 7D and 7J) in UCP3 knock-out mice compared to wild-type control mice.

Comparing the data for the effect of starvation on the relative proportion of thymocytes from wild-type mice, it appears there is a 30% increase in the proportion of CD4SP cells in wild-type mice (Fig. 7C and 7I, $p=0.00031$), a 50% increase in the number of CD8SP in wild-type mice (Fig. 7D and 7J, $p=0.001$), a 42% increase in proportion of DN (Fig. 7E and 7K, $p=0.004$) and a 6% decrease in the proportion of DP cells in wild-type mice (Fig. 7F and 7L, $p=0.003$) in wild-type animals. The effect of starvation on UCP3

knock-out mice saw a 2.3-fold increase ($p=0.001$) in CD4SP cells (Fig. 7C and 7I), no significant effect on CD8SP (Fig. 7D and 7J) or DN cells (Fig. 7E and 7K), and a small 4% reduction in DP (Fig. 7F and 7L, $p=0.015$) in a comparison of fed and starved UCP3 knock-out mice.

Figure 8A-F displays the relative proportion of splenocytes, in a comparison of wild-type and UCP3 knock-out (UCP3^{-/-}) mice in the fed state, that are CD4SP lymphocytes, CD8SP lymphocytes, DP lymphocyte and other cells (including monocytes, natural killer cells, B-lymphocytes). The data demonstrates that there is a significant ($p=0.0001$) 2-fold increase in the abundance of CD4SP (Fig. 8C), 2-fold increase in the abundance of CD8SP (Fig. 8D, $p=0.0001$) and 2-fold increase in the abundance of DP (Fig. 8F $p=0.0001$) in the spleens of UCP3 knock-out mice compared to wild-type controls. There is small but significant ($p=0.0006$) increase in the amount of “other cells” in wild-type compared to UCP3 knock-out mice (Fig. 8E). Representative dot-plots for splenocytes from fed wild-type and UCP3^{-/-} are shown (Fig. 8A and 8B). Figure 8G-L displays the proportion of splenocytes, that are CD4SP lymphocytes, CD8SP lymphocytes, DP lymphocyte and other cells (including monocytes, natural killer cells, B-lymphocytes), in a comparison of wild-type and UCP3 knock-out mice in the fasted state. The data demonstrates that there is a significant ($p=0.02$) 2-fold decrease in the relative abundance of DP cells in UCP3 knock-out mice compared to wild-type controls (Fig. 8L), with no significant difference in the relative abundance of CD4SP (Fig. 8I), CD8SP (Fig. 8J), and other cells (Fig. 8K) in wild-type compared to UCP3 knock-out mice. Representative dot-plots for splenocytes from fasted wild-type and UCP3 knock-out mice are shown (Fig. 8G and 8H).

Comparing the data from the fed and fasted states and whether there is any effect on the relative proportion of splenocyte subsets from UCP3 knock-out and wild type mice it would appear that starvation attenuates any aforementioned differences in the abundance of CD4SP (Fig. 8C and 8I), CD8SP (Fig. 8D and 8J) and other cells (Fig. 8E and 8K), while causing a 4-fold swing (Fig. 8F and 8L) in the proportion on DP cells in UCP3 knock-out mice compared to wild-type control mice.

Comparing the data for the effect of starvation on the relative proportion of splenocytes from wild-type mice, it appears there is a doubling in the proportion of CD4SP cells in wild-type mice (Fig. 8C and 8I $p=0.001$), a quadrupling in the number of CD8SP in wild-type mice (Fig. 8D and 8J, $p=0.001$), an

approximate tripling of the proportion of other cells (Fig. 8E and 8K, $p=0.0006$) and a tripling in the proportion of DP cells in wild-type mice (Fig. 8F and 8L, $p=0.001$) in wild-type animals. The effect of starvation on UCP3 knock-out mice was less marked, with no significant effect on the proportion of CD4SP (Fig. 8C and 8I), CD8SP (Fig. 8D and 8J) and other cells (Fig. 8E and 8K), but a 50% reduction in DP (Fig. 8F and 8L, $p=0.02$) in a comparison of fed and starved UCP3 knock-out mice.

We conclude that lack of UCP3 effects the relative abundance of all splenocyte subsets compared to those from wild-types, that starvation attenuates these differences and that starvation has a more marked effect on the proportion of splenocyte subsets from wild-type than it does from mice lacking UCP3.

Figure 9A and 9B compares the relative percentage apoptosis occurring in thymocytes isolated from 3 week old wild-type mice and 3 week old UCP3 knock-out mice after 5 hour treatment with $1\mu\text{M}$ dexamethasone or vehicle (ethanol). There is no significant difference in the extent of apoptosis in dexamethasone- treated thymocytes isolated from fed UCP3 knock-out mice or fed wild-type mice (Fig. 9A). However, the level of spontaneous apoptosis occurring in the thymocytes of fed wild-type mice is 1.3-fold less than in the thymocytes from fed UCP3 knock-out mice ($p=0.05$)(Fig. 9A). Starvation did not manifest any significant difference in the extent of apoptosis in dexamethasone- treated thymocytes isolated from fed UCP3 knock-out mice or fed wild-type mice (Fig. 9B). However, the level of spontaneous apoptosis occurring in the thymocytes of fasted wild-type mice persisted at 1.3-fold less than in the thymocytes from fed UCP3 knock-out mice ($p=0.003$)(Fig. 9B). Analysis of apoptosis in thymocytes from starved animals revealed a dramatic increase in the apoptotic potential of the thymocytes from both wild-type and UCP3 knock-out mice, with an approximate 3-fold increase in apoptosis following dexamethasone treatment in thymocytes from wild-type and UCP3 knock-out mice (Fig. 9A and 9B), and an approximate 4-5-fold increase in apoptosis in thymocytes from wild-type and UCP3 knock-out mice treated with vehicle (Fig. 9A and 9B). However, the relative proportion of cells undergoing apoptosis, in the fed and fasted state, in a comparison of wild-type and UCP3 knock-out mice was not affected by starvation. No significant differences were observed in caspase 3 or caspase 7 activity in a comparison of thymocytes from wild-type or UCP3 knock-out mice, either in the presence of dexamethasone or vehicle after 5 hours (results not

shown). Similar data to those already detailed for measurements at 5 hours on the relative proportion of thymocytes undergoing apoptosis were observed for splenocytes incubated for 18h (results not shown).

Figure 9C and 9D compares the relative percentage apoptosis occurring in all splenocytes isolated from 3 week old wild-type mice and 3 week old UCP3 knock-out mice after 5 hour treatment with 1 μ M dexamethasone or vehicle (ethanol). There is no significant difference in the extent of apoptosis in dexamethasone- treated thymocytes isolated from fed UCP3 knock-out mice or fed wildtype mice (Fig. 9C). Similarly, the level of spontaneous apoptosis occurring in the splenocytes of fed wild-type mice is only 1.4-fold greater than in the splenocytes from fed UCP3 knock-out mice ($p=0.005$)(Fig. 9C). Analysis of apoptosis in splenocytes from starved animals revealed a increase in the apoptotic potential of the splenocytes from both wild-type and UCP3 knock-out mice, with an approximate 2-fold increase in apoptosis following dexamethasone treatment in splenocytes from wild-type and a 2.5-fold increase in UCP3 knock-out mice (Fig. 9C and 9D), and an approximate 4-5-fold increase in apoptosis in splenocytes from wild-type and UCP3 knock-out mice treated with vehicle (Fig. 9C and 9D). However, the relative proportion of cells undergoing apoptosis, in the fed and fasted state, in a comparison of wild-type and UCP3 knock-out mice was affected by starvation following drug treatment, with 1.25-fold increase in dexamethasone treated cells (Fig. 9C versus 9D). There was no real change in the relative proportion of cells from wild-type and UCP3 knock-out mice undergoing apoptosis in vehicle treated cells (Fig. 9C versus 9D).

Similar data on the relative proportion of splenocytes undergoing apoptosis were observed for splenocytes incubated for 18h (results not shown).

4. DISCUSSION

Our data in figure 1 demonstrate that UCP3 is present in both thymus and spleen mitochondria of mice. These data endorse data previously reported, by us, for the presence of UCP3 in thymus and spleen of rats [2], and emphasize the selectivity of our antibody to UCP3 over other mitochondrial transporters/proteins. The selectivity of the antibody is further emphasized by the demonstration of UCP3 in thymocytes from wild-type mice with no detection in UCP3 knock-out mice (Fig. 2). Furthermore, UCP3 is present in mitochondria of thymus and spleen up to at least 16 weeks after birth (Fig. 3). Interestingly, levels of UCP3

drop by about a half in thymus and a fifth in spleen after three weeks, as reflected in their mitochondria. This time period coincides with a switch by mice from suckling to weaning, and the reduction in UCP3 level most probably reflects this change, with the interesting conclusion that suckling results in maintenance of a higher UCP3 level than weaning. Similar observations were made at this same time period for constitutively expressed UCP1 in thymus mitochondria [22].

UCP3 has long been associated with lipid metabolism [7] and there have been several reports in the literature demonstrating that UCP3 protein expression increases in skeletal muscle on starvation of animals [2,5]. In this study, we observed that UCP3 expression was starvation sensitive in mouse thymus, increasing ~3-fold per unit mass of mitochondria (Fig. 4). However, UCP3 expression was unaffected by starvation in spleen of mouse (Fig. 4), although there may be a moderate fractional increase in UCP3 in the T-lymphocyte subset as reflected in rat [14]. So clearly there is a differential sensitivity of UCP3 to starvation in thymus and spleen.

Despite the absence of UCP3 in knock-out mice there is no significant difference in thymus weight in a comparison with thymi from wild-type mice in the fed state and or fasted state (Fig. 5). However, as has been previously reported [34], there is a significant reduction in thymus mass due to starvation in wild-type mice and this holds true for UCP3 knock-out mice also. The lack of difference in thymus mass in a comparison of wild-type mice and UCP3 knock-out mice, yet a reduction in thymus mass on starvation, is also reflected at the level of total cell abundance. A similar picture emerges for spleens of UCP3 knock-out mice in that there is no significant difference in spleen mass in a comparison the thymi from wild-type in the fed state (Fig. 5). However, there is a significant modest reduction in spleen mass in the absence of UCP3 in the fasted state. Starvation had no significant effect on spleen mass of wild-type fed mice nor was there a reduction in the spleen mass of starved UCP3 knock-out mice. The profile with regard to spleen mass is also reflected at the cell number level.

Using oxygen consumption as an index of cellular metabolism and mitochondrial function we observed no apparent effect of the absence of UCP3 on total thymocyte or splenocyte oxygen consumption rates, or oxygen consumption rates due to proton leak, fasting the animals had no effect of the aforementioned comparisons (Fig. 6). If UCP3 was to have an effect on cellular metabolism, as measured in vitro, under the

conditions defined here, one might expect any potential difference between cells from wild-type and UCP3 knock-outs or between cells from wild-type from fed and fasted animals to be manifest in the comparisons. Having said that, there may have been an effect of the absence of UCP3 on thymocytes or splenocytes *in vivo* which may have been lost in our subsequent *in vitro* oxygen consumption analysis.

While not reflected as a difference in total cell numbers (Fig. 5), there does appear to be a difference in the proportional of certain subsets of thymocytes as a result of the lack of UCP3 compared to those from wild-types in the fed state (Fig. 7). Lack of UCP3 manifests as reduced CD4⁺ single positive cells and reduced double negative cells in the thymus, but these differentials are not exacerbated by starvation. However, starvation does increase the proportion CD8⁺ in animals in wild-types compared to UCP3 knock-out mice (Fig. 7). Again, there does appear to be a difference in the proportional of certain subsets of thymocytes as a result of starvation within wild-type and UCP3 groups without a difference in total cell numbers. Within wild-type mice starvation results in an increase in the proportion the smaller subsets namely CD4SP, CD8SP and DN cells which in turn are offset by a 6% decrease in the proportion of the most predominant DP cells. In UCP3 knock-out mice after starvation we observed a different profile with a significant increase in CD4SP cells only, which in turn was offset by and a small reduction in most prevalent DP cells (Fig. 7). Overall we can conclude that UCP3 does affect thymocyte cell profile in the fed and fasted state.

Lack of UCP3 in the spleen of fed animals manifests as a 2-fold increase in the proportion of CD4⁺, CD8⁺ and DP cells (Fig. 8) and this is against a backdrop of no significant different in total cell numbers (Fig. 6). Starvation attenuates these proportionate differences in a comparison of wild-type and UCP3 knock-out mice (Fig. 8) while causing a 4-fold swing in the proportion on DP cells in the spleen of UCP3 knock-out mice compared to wild-type control mice. Clearly any changes in the proportion of cell populations in the spleen in wild-type versus UCP3 knock-out animals as a result of starvation must directly result from changes in the thymus as UCP3 abundance is unaffected by starvation in the spleen but is affected in the thymus and T-lymphocytes in the spleen originate from the thymus. The consequence is a greater proportion of double positive cells in the periphery (spleen) which is indicative of a processing alteration/problem in the thymus of UCP3 knock-out mice.

Furthermore, starvation has much more dramatic effect on wild-type mice splenocyte profile than on that of UCP3 knock-out mice (Fig. 8). While in wild-type mice starvation increased CD4SP, CD8SP, DP and other cells, the effect of starvation on UCP3 knock-out mice was less marked, with no significant effect on the proportion of CD4SP, CD8SP, and other cells and a reduction in DP (Fig. 8). We conclude that lack of UCP3 affects the relative abundance of all splenocyte subsets compared to those from wild-types, that starvation attenuates these differences and that starvation has a more marked effect on the proportion of splenocyte subsets from wild-type than it does from mice lacking UCP3. Furthermore, the difference in the splenocyte profiles in a comparison of fed and fasted wild-type mice must be as a result of UCP3 manifesting its effect in the thymus as UCP3 abundance is unaffected by starvation in the spleen, but is affected in the thymus and T-lymphocytes in the spleen originate from the thymus.

As apoptosis is a prevalent event in thymus in both positive and negative selection processes for thymocytes, we compared the apoptotic potential of thymocytes lacking UCP3 with thymocytes from wild-type mice (Fig. 9). The observations of increased apoptotic potential with vehicle alone, in UCP3 knock-out mice relative to wild-type mice in both fed and fasted state, are reflected in the tendency for a decreased splenocyte cell number in the fed state and the significant decrease in splenocyte numbers after starvation (Fig. 6), because no significant difference in the thymus cell numbers are evident (Fig. 5). Clearly splenocytes from UCP3 knock-out mice are more resistant to apoptosis with vehicle alone in the fed state, and with dexamethasone and vehicle in the fasted state, than those from wild-type mice (Fig. 9), however there was no real difference in the proportion of cells undergoing apoptosis in wild-type versus UCP3 knock-out mice in the transition from fed to fasted state. So we conclude that UCP3 has an impact on apoptotic potential splenocytes, but the UCP3 dependent effect is not exacerbated by starvation. What is strikingly evident from the data in Figure 9 is the dramatic increase in apoptosis of thymocytes and splenocytes upon starvation of the wild-type or UCP3 knock-out animals.

There have been two other studies looking at the effect on UCP ablation of thymocyte profile. Krauss et al. [26] observed no significant differences on thymocyte profile in a comparison of wild-type and UCP2 knock-out mice (in the fed state). Adams et al. [22] demonstrated a ~3-fold reduction in spleen cell numbers, a halving of CD8 single positive cell numbers in thymus and a significant incremental increase in CD4/CD8

double positives cell numbers in UCP 1 knock-out mice compared to wild-type mice (in the fed state). In a comparison of wild-type and UCP3 knock-out mice none of the aforementioned parameters were affected, indicating different role for UCP1 and UCP3 in thymus. On the other hand, in spleens of UCP1 knock-out mice there was an approximate halving of CD8 single positive cell numbers and a doubling of CD4/CD8 double positive cell numbers compared to wild-type mice. In this study conversely to the former, we see a doubling of CD8 single positive cells, but consistent with the latter we see a doubling of CD4/CD8 double positive cells in UCP3 knock-out mice compared to wild-types.

We conclude that constitutively expressed UCP3 is a factor in determining T-cell population selection in mice.

Acknowledgements

Acknowledgements: Funding for this study was provided by a Trinity College Studentship stipend to O. Kelly, a Science Foundation Ireland Principal Investigator award (SFI 06/IN.1/B67) to R.K. Porter is a member of the MITOFOOD COST Action (FA0602).

REFERENCES

- [1] O. Boss, S. Samec, A. Paoloni-Giacobino, C. Rossier, A. Dulloo, J. Seydoux, P. Muzzin, J.P. Giacobino, Uncoupling protein-3: a new member of the mitochondrial carrier family with tissue-specific expression, *FEBS Lett*, 408 (1997) 39-42.
- [2] O. Cunningham, A.M. McElligott, A.M. Carroll, E.P. Breen, C. Reguenga, M.E.M. Oliveira, J.E. Azevedo, R.K. Porter, Selective detection of UCP3 expression in skeletal muscle: effect of thyroid status and temperature acclimation. *Biochim. Biophys. Acta* 1604 (2003) 170 - 179.
- [3] S. Krauss, C. Zhang and B.B. Lowell, The mitochondrial uncoupling protein homologues, *Nat. Rev. Mol. Cell. Biol.* 6 (2005) 248-261.

- [4] S, Samec, J. Seydoux, A.G. Dulloo, Role of UCP homologues in skeletal muscles and brown adipose tissue: mediators of thermogenesis or regulators of lipids as fuel substrate? *FASEB J.* 12(1998) 715-724.
- [5] S. Cadenas, J.A. Buckingham, S. Samec, J. Seydoux, N. Din, A.G. Dulloo, M.D. Brand, UCP2 and UCP3 rise in starved rat skeletal muscle but mitochondrial proton conductance is unchanged, *FEBS Lett.* 462 (1999) 257-260.
- [6] O. Boss, S. Samec, F. Kuhne, P. Bijlenga, F. Assimacopoulos-Jeannet, J. Seydoux, J. P. Giacobino, P. Muzzin, Uncoupling protein-3 expression in rodent skeletal muscle is modulated by food intake but not by changes in environmental temperature, *J. Biol. Chem.* 273 (1998) 5-8.
- [7] A.G. Dulloo, S. Samec Uncoupling proteins: their roles in adaptive thermogenesis and substrate metabolism reconsidered, *Br. J. Nutr.* 86 (2001) 123-139.
- [8] A. Lombardi, R.A. Busiello, L. Napolitano, F. Cioffi, M. Moreno, P. de Lange, E. Silvestri, A. Lanni, F. Goglia, UCP3 translocates lipid hydroperoxide and mediates lipid hydroperoxide dependent mitochondrial uncoupling, *J. Biol. Chem.* 285 (2010) 16599-16605.
- [9] K.S. Echtay, D. Roussel, J. St-Pierre, M.B. Jekabsons, S. Cadenas, J.A. Stuart, J.A. Harper, S.J. Roebuck, A. Morrison, S. Pickering, J.C. Clapham, M.D. Brand, Superoxide activates mitochondrial uncoupling proteins, *Nature* 415 (2002) 96-99.
- [10] K.S. Echtay, T.C. Esteves, J.L. Pakay, M.B. Jekabsons, A.J. Lambert, M. Portero-Otin, R. Pamplona, A.J. Vidal-Puig, S. Wang, S.J. Roebuck, M.D. Brand, A signalling role for 4-hydroxy-2-nonenal in regulation of mitochondrial uncoupling, *EMBO J.* 22 (2003) 4103-4110.
- [11] I.G. Shabalina, N. Petrovic, T.V. Kramarova, J. Hoeks, B. Cannon, J. Nedergaard, UCP1 and defense against oxidative stress. 4-hydroxy-2-nonenal effects on brown fat mitochondria are uncoupling protein 1-independent, *J. Biol. Chem.* 281 (2006) 13882-13893.
- [12] A.J. Robinson, C. Overy, E.R. Kunji, The mechanism of transport by mitochondrial carriers based on analysis of symmetry, *Proc. Natl. Acad. Sci.* 105 (2008) 17766-17771.
- [13] S. Enerbäck, A. Jacobsson, E.M. Simpson, C. Guerra, H. Yamashita, M-E. Harper, L.P. Kozak, Mice lacking mitochondrial uncoupling protein are cold-sensitive but not obese, *Nature* 387 (1997) 90-94.

- [14] A.M Carroll, R.K. Porter, Starvation sensitive UCP3 expression in rat thymus and spleen, *Biochim. Biophys. Acta* 1700 (2004) 145-150.
- [15] M.F. Essop, P. Razeghi, C. McLeod, M.E Young, H. Taegtmeier, M.N Sack, Hypoxia-induced decrease of UCP3 gene expression in rat heart parallels metabolic gene switching but fails to affect mitochondrial respiratory coupling, *Biochem. Biophys. Res. Commun.* 314 (2004) 561-556.
- [16] **C.J. Chou, M.C. Cha, D.W. Jung , C.N. Boozer, S.A. Hashim, F.X. Pi-Sunyer, High-fat diet feeding elevates skeletal muscle uncoupling protein 3 levels but not its activity in rats. *Obes. Res.* 9 (2001) 313-319.**
- [17] D.W. Gong, S. Monemdjou, O. Gavrilova, L.R. Leon, B. Marcus-Samuels, C.J. Chou, C. Everett, L.P. Kozak, C. Li, C. Deng, M.E. Harper, M.L. Reitman, Lack of obesity and normal response to fasting and thyroid hormone in mice lacking uncoupling protein-3, *J. Biol. Chem.* 275 (2000) 16251-16257.
- [18] A.J. Vidal-Puig, D. Grujic, C.Y. Zhang, T. Hagen, O. Boss, Y. Ido, A. Szczepanik, J. Wade, V. Mootha, R. Cortright, D.M. Muoio, B.B. Lowell, Energy metabolism in uncoupling protein 3 gene knockout mice, *J. Biol. Chem.* 275 (2000) 16258-16266.
- [19] A.M. Carroll, L.R. Haines, T.W. Pearson, P. Fallon, C. Walsh, C.M. Brennan, E.P. Breen, R.K. Porter, Detection of a functioning UCP 1 in Thymus, *J. Biol. Chem.* 280 (2005) 15534-15543.
- [20] A.E. Adams, O. Hanrahan, D.N. Nolan, H.P. Voorheis, P. Fallon, R.K. Porter, Images of mitochondrial UCP 1 in mouse thymocytes using confocal microscopy. *Biochim. Biophys. Acta* 1777 (2007) 115-117.
- [21] A.E. Adams, A.M. Carroll, P.G. Fallon, R.K. Porter, Mitochondrial uncoupling protein 1 expression in thymocytes, *Biochim. Biophys. Acta* 1777 (2008) 772-776.
- [22] A.E. Adams, O.M. Kelly, R.K. Porter, Absence of mitochondrial uncoupling protein 1 affects apoptosis in thymocytes, thymocyte/T-cell profile and peripheral T-cell number, *Biochim Biophys. Acta.* 1797 (2010) 807-816.
- [23] D. Arsenijevic, H. Onuma, C. Pecqueur, S. Raimbault, B. Manning, B. Miroux, E. Couplan, M. Alves-Guerra, M. Goubern, R. Surwit, F. Bouillaud, D. Richard, S. Collins, D. Ricquier, Distribution of the

- uncoupling protein-2 gene in mice reveals a role in immunity and reactive oxygen species production. *Nat. Genet.* 26 (2000) 435-439.
- [24] Y. Bai, H. Onuma, X. Bai, A.V. Medvedev, M. Misukonis, J.B. Weinberg, W. Cao, J. Robidoux, L.M. Floering, K.F. Daniel, S. Collins, Persistent NF- κ B activation in UCP2^{-/-} mice leads to enhanced nitric oxide and inflammatory cytokine production, *J. Biol. Chem.* 280 (2005) 19062-19069.
- [25] Y. Emre, T. Nübel, Uncoupling protein UCP2: When mitochondrial activity meets immunity, *FEBS Letts* 584 (2010) 1437-1442.
- [26] S. Krauss, C.Y. Zhang, B.B. Lowell, A significant portion of mitochondrial proton leak in intact thymocytes depends on expression of UCP2, *Proc. Natl. Acad. Sci.* 99 (2002) 118-122.
- [26] T.K. Starr, S.C. Jameson, K.A. Hogquist, Positive and negative selection of T cells, *Annu. Rev. Immunol.* 21 (2003) 139-176.
- [27] J. C. Zúñiga-Pflücker, T-cell development made easy, *Nature Rev. Immunol.* 4, (2004) 67-72.
- [28] A.C. Hayday, D.J. Pennington, Key factors in the organized chaos of early T-cell development, *Nature Immunol.* 8 (2007) 137-144
- [29] K.H.G Mills, in A. Robinson, G. Farrar, C. Wilbin (Eds.), *Methods in Molecular Medicine – Vaccine protocols*, Humana Press, New Jersey, 1996, pp197-221.
- [30] R.E. Mebius, G. Kraal, Structure and function of the spleen, *Nature Rev. Immunol.* 5 (2005) 606-616.
- [31] F. Buttgerit, M.D. Brand, A hierarchy of ATP-consuming processes in mammalian cells, *Biochem. J.* 312 (1995) 163-167.
- [32] J.B. Chappell, R.G. Hansford, in: G.D. Birnie (Ed.), *Subcellular Components: Preparation and Fractionation*, Butterworths, London, 1972, pp. 77 – 91.
- [33] P.K. Smith, R.I. Krohn, G.T. Hermanson, A.K. Mallia, F.H. Gartner, M.D. Provenzano, E.K. Fujimoto, N.M. Goeke, B.J. Olson, D.C. Klenk, Measurement of protein using bicinchoninic acid, *Anal. Biochem.* 150 (1985) 76-85.
- [34] **J.K. Howard, G. M. Lord, G.Matarese, S. Vendetti, M.A. Ghatei, M. A. Ritter, R. I. Lechler, S. R. Bloom, Leptin protects mice from starvation-induced lymphoid atrophy and increases thymic cellularity in *ob/ob* mice, *J. Clin. Invest.* 104 (1999) 1051–1059.**

Figure 1. Detection of UCP3 in thymus and spleen mitochondria. Our polyclonal peptide antibody raised to UCP3 (custom made by Eurogentec and previously characterized in Cunningham et al. [2]) detects UCP3 in both lysates from yeast over-expressing UCP3 (A) and (C) and mitochondria isolated from thymus (A) and spleen (C) of wild-type mice. No UCP3 was detected in UCP3 knockout mice or in mouse liver mitochondria, as expected (A) and (C). An independent marker of mitochondria in (B) thymus and (D) spleen preparations was confirmed using an antibody to pyruvate dehydrogenase subunit E1 α (Mitosciences).

Figure 2. Confocal microscopy images of UCP3 in thymocytes from wild-type and UCP3 knock-out mice. The images show localisation of the nucleus within thymocytes from wild-type and UCP3 knock-out mice using Hoechst stain the labelled surface marker Thy 1 (green), UCP3 detected using our peptide antibody for UCP3 and a secondary antibody conjugated to Alexa 647 (red) and phase contrast images of thymocytes from wild-type and UCP3^{-/-} mice. Bar is 5 μ m.

Figure 3. Age-dependent profile of UCP3 expression in mitochondria isolated from thymus and spleen of wild-type mice. The abundance of constitutively expressed UCP3 in (A) thymus and (D) spleen was measured in wild-type mice aged 1, 2, 3, 4, 6, 8 and 16 weeks, with liver mitochondria as a negative control. Pyruvate dehydrogenase subunit E1 α was used as an independent marker of mitochondria in (B) thymus and (E) spleen preparations. Collated densitometry data from immunoblots for (C) thymus and (D) spleen mitochondria are plotted relative to PDH abundance for 3 separate experiments and is expressed as mean \pm sem.

Figure 4. The effect of starvation of UCP3 expression in thymus and spleen. The abundance of constitutively expressed UCP3 in (A) thymus and (D) spleen was measured in wild-type mice following 24-

hour fasting, with liver mitochondria as a negative control. Pyruvate dehydrogenase subunit E1 α was used as an independent marker of mitochondria in (B) thymus and (E) spleen preparations. Collated densitometry data from immunoblots for (C) thymus and (D) spleen mitochondria are plotted relative to PDH abundance for 3 separate experiments, expressed as mean \pm sem. Key: N.S. = not significant.

Figure 5. Comparison of thymus and spleen mass and cell number from wild-type (■) and UCP3 knock-out (□) in the fed and fasted state. (A) Thymus and spleen (B) tissue mass from wild-type and UCP3 knock-out mice in the fed and fasted state, were measured. Total cell count from the (C) thymus and (D) spleen from wild-type mice and UCP3 knock-out mice in the fed and fasted state are given (C). Data are from 3 separate experiments, performed in at least triplicate and expressed as mean \pm sem.

Figure 6. Oxygen consumption rates in thymocytes and splenocytes from wild-type and UCP3 knock-out mice in the fed state and wild-type mice in the fed and fasted state. Oxygen consumption rates (nmolesO₂/min/10⁶cells) by (A) thymocytes and (B) splenocytes isolated from wild-type (■) and UCP3 knock-out (□) mice in the fed are compared together with data from a separate set of experiments comparing oxygen consumption of (C) thymocytes and (D) splenocytes in the fed (black) and fasted (grey) state. Oligomycin was added to determine the oxygen consumption due to the proton leak of the in situ mitochondria (Leak). FCCP was added to determine the maximal electron chain activity of the in situ mitochondria. Data are from 3 separate experiments, performed in at least triplicate and expressed as mean \pm sem where n=3. Key: N.S. = not significant.

Figure 7. FACS analysis data for the relative abundance of CD4 single positive (CD4SP), CD8 single positive (CD8SP), CD4CD8 double negative (DN) and CD4CD8 double positive (DP) from thymocytes of wild-type (WT) and UCP3 knock-out (UCP3^{-/-}) mice in the fed state and fasted state. Representative dot-plots for thymocytes from fed wild-type (A), fed UCP3^{-/-} (B), fasted wild-type (G) and fasted UCP3^{-/-} (H) are shown. Collated data from at least three determination are given for the abundance of (C) CD4SP, (D) CD8SP, (E) DN and (F) DP cells from thymocytes of wild-type (WT) and UCP3 knock-out (UCP3^{-/-})

mice in the fed state and (I) CD4SP, (J) CD8SP, (K) DN and (L) DP cells from thymocytes of wild-type (WT) and UCP3 knock-out (UCP3^{-/-}) mice in the fasted state. N.S. = not significant.

Figure 8. FACS analysis data for the relative abundance of CD4 single positive (CD4SP), CD8 single positive (CD8SP), non-T-lymphocytes (other cells) and CD4CD8 double positive (DP) from splenocytes of wild-type (WT) and UCP3 knock-out (UCP3^{-/-}) mice in the fed state and fasted state. Representative dot-plots for splenocytes from fed wild-type (A), fed UCP3^{-/-} (B), fasted wild-type (G) and fasted UCP3^{-/-} (H) are shown. Collated data from at least three determination are given for the abundance of (C) CD4SP, (D) CD8SP, (E) Other cells and (F) DP cells from splenocytes of wild-type (WT) and UCP3 knock-out (UCP3^{-/-}) mice in the fed state and (I) CD4SP, (J) CD8SP, (K) other cells and (L) DP cells from splenocytes of wild-type (WT) and UCP3 knock-out (UCP3^{-/-}) mice in the fasted state. N.S. = not significant.

Figure 9. The relative level of apoptosis in thymocytes and splenocytes from wild-type mice (WT) and UCP3 knock-out mice (UCP3^{-/-}) in the fed and fasted state. The degree of apoptosis, after 5 hour treatment with 1 μ M dexamethasone or vehicle (ethanol), in thymocytes from wild-type mice and UCP3 knock-out mice in the (A) fed and (B) fasted state and in splenocytes from wild-type mice and UCP3 knock-out mice in the (C) fed and (D) fasted state, was determined using Annexin V binding and propidium iodide. N.S. = not significant.

Figure 1

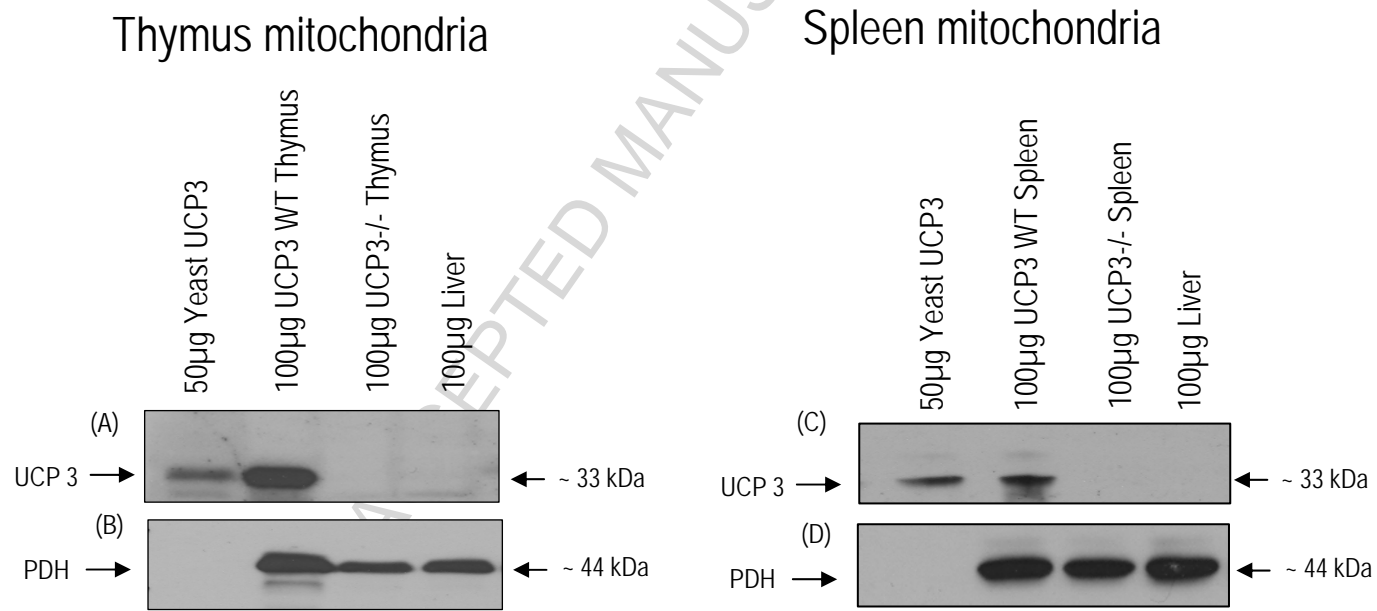


Figure 2

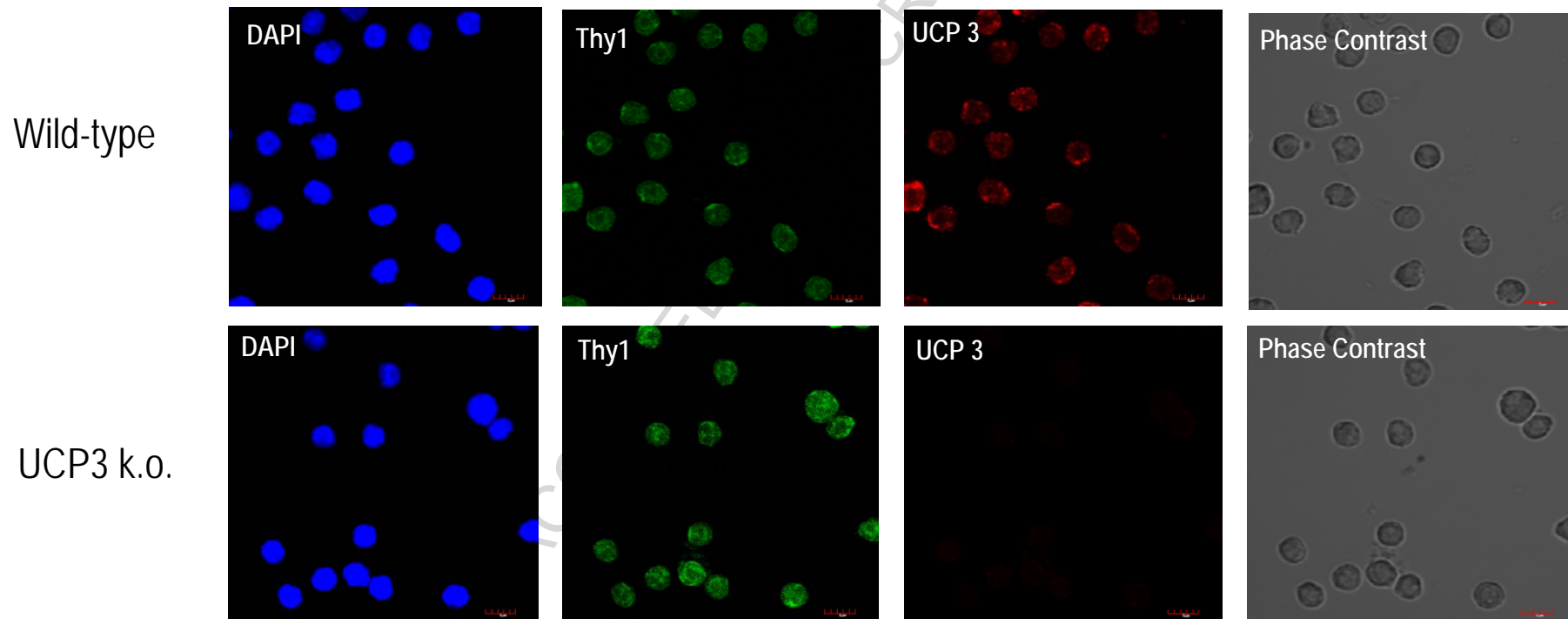
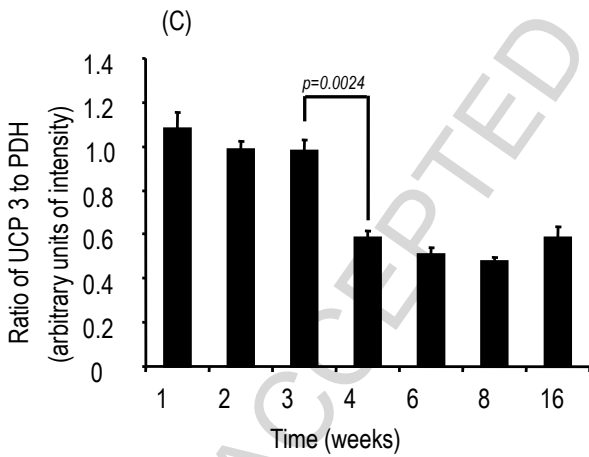
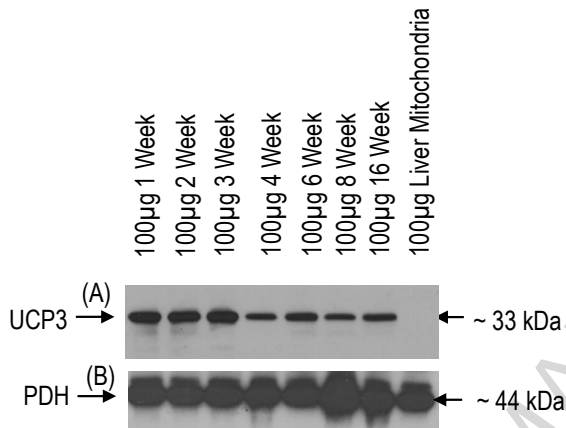


Figure three

Thymus mitochondria



Spleen mitochondria

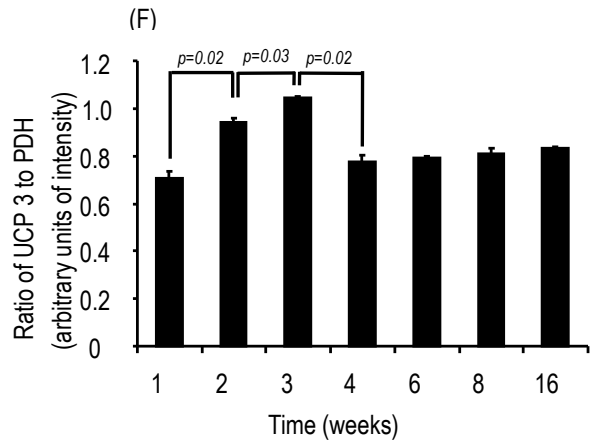
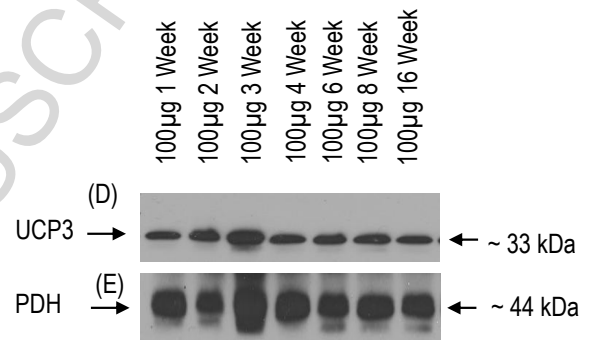


Figure 4

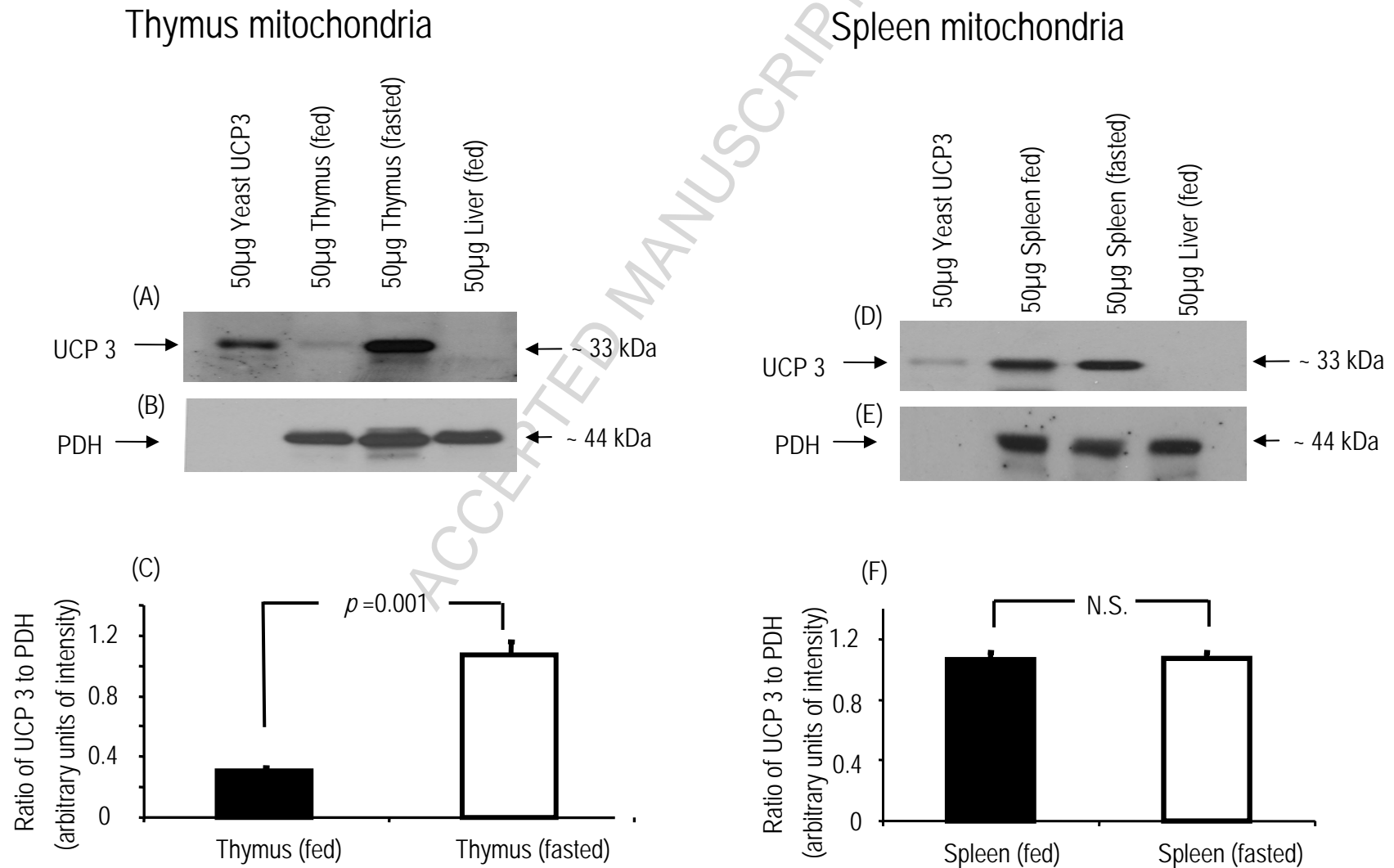
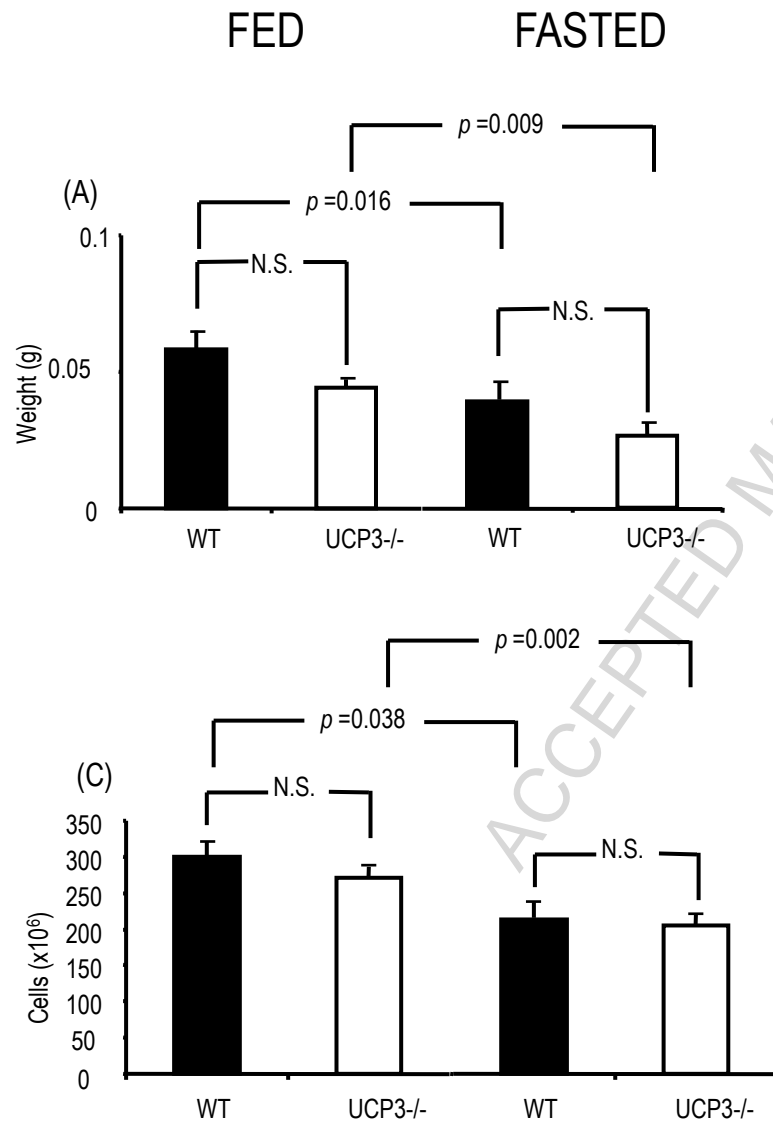


Figure five

Thymus



Spleen

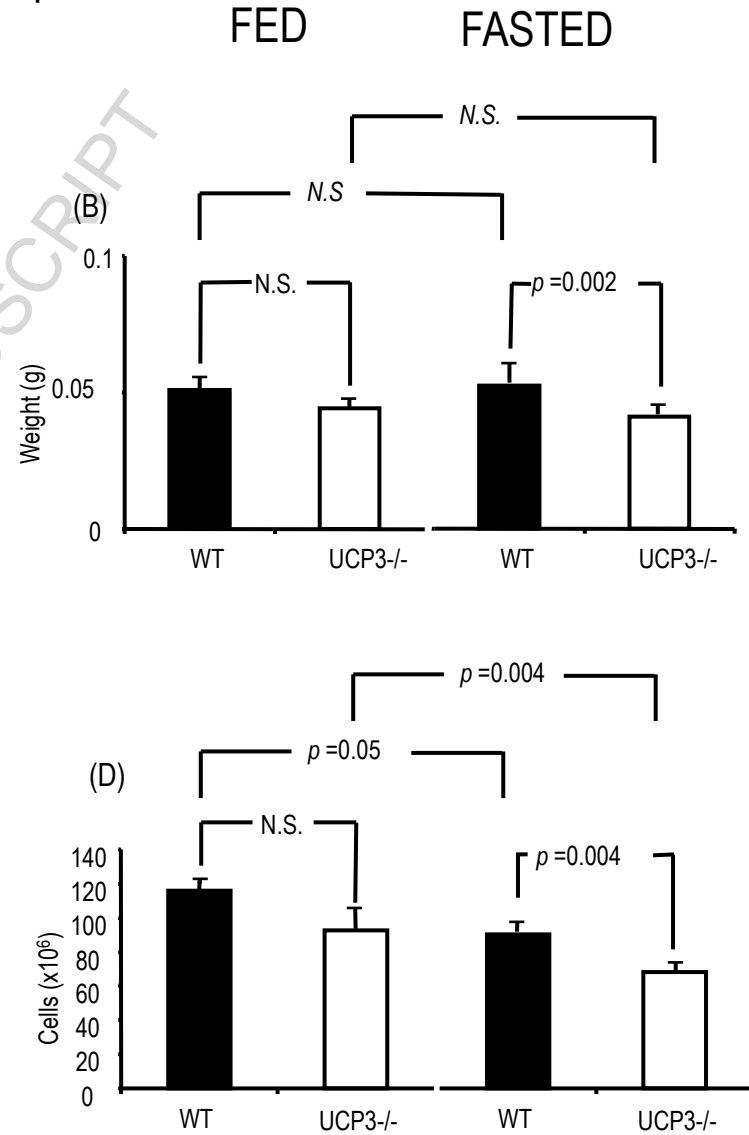
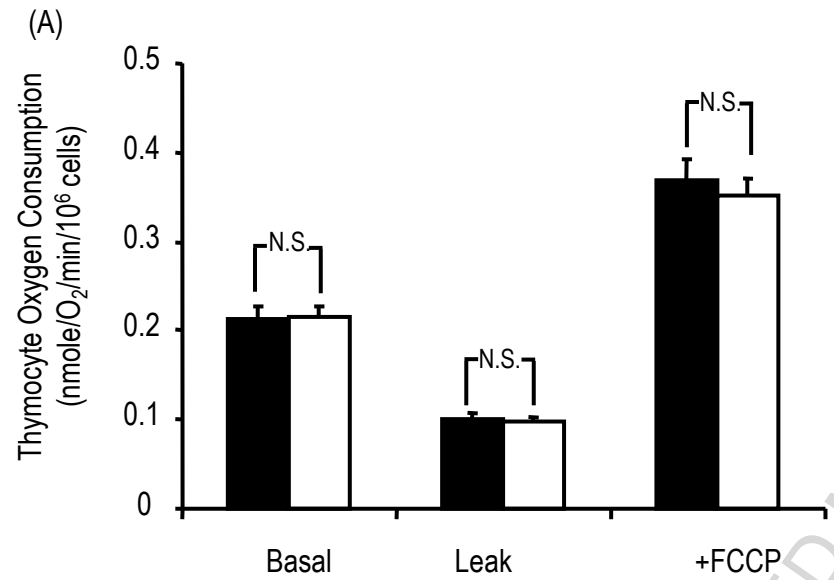


Figure six

Thymus



Spleen

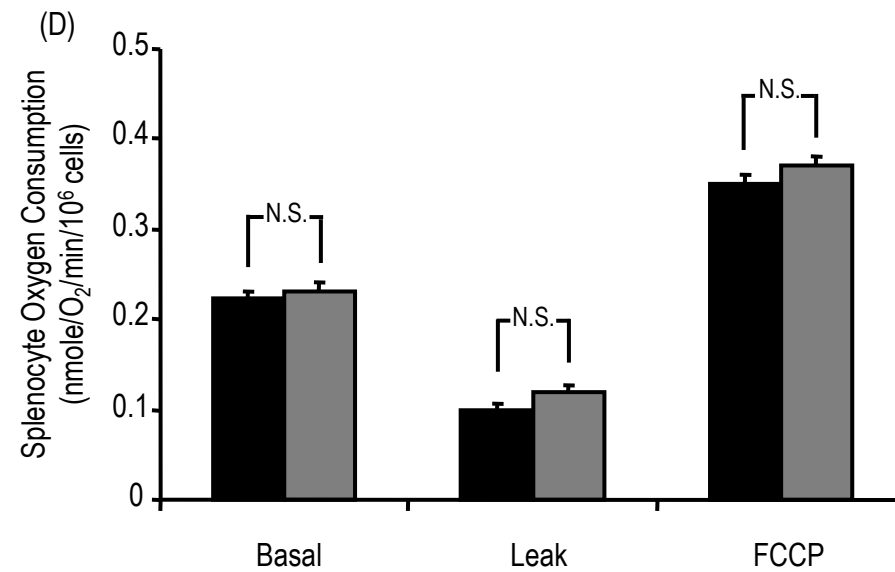
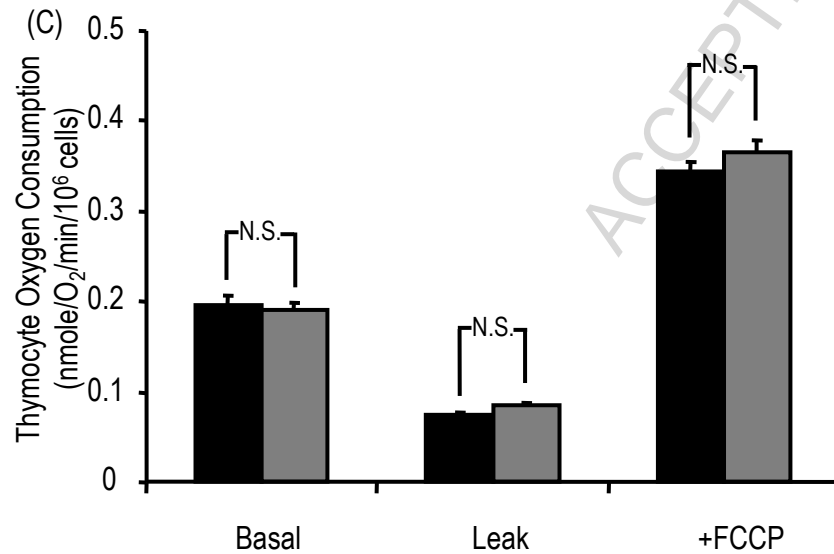
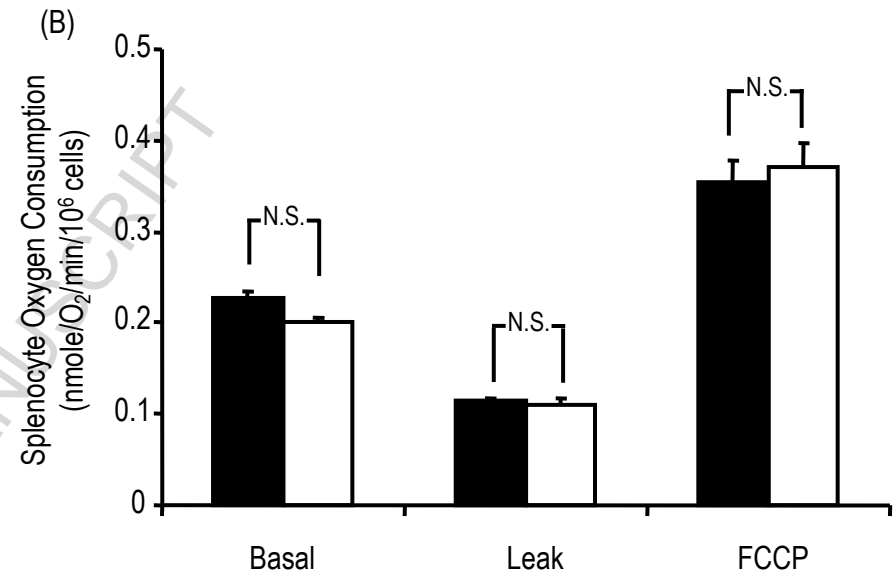


Figure 7

Thymocytes: FED

Thymocytes: FASTED

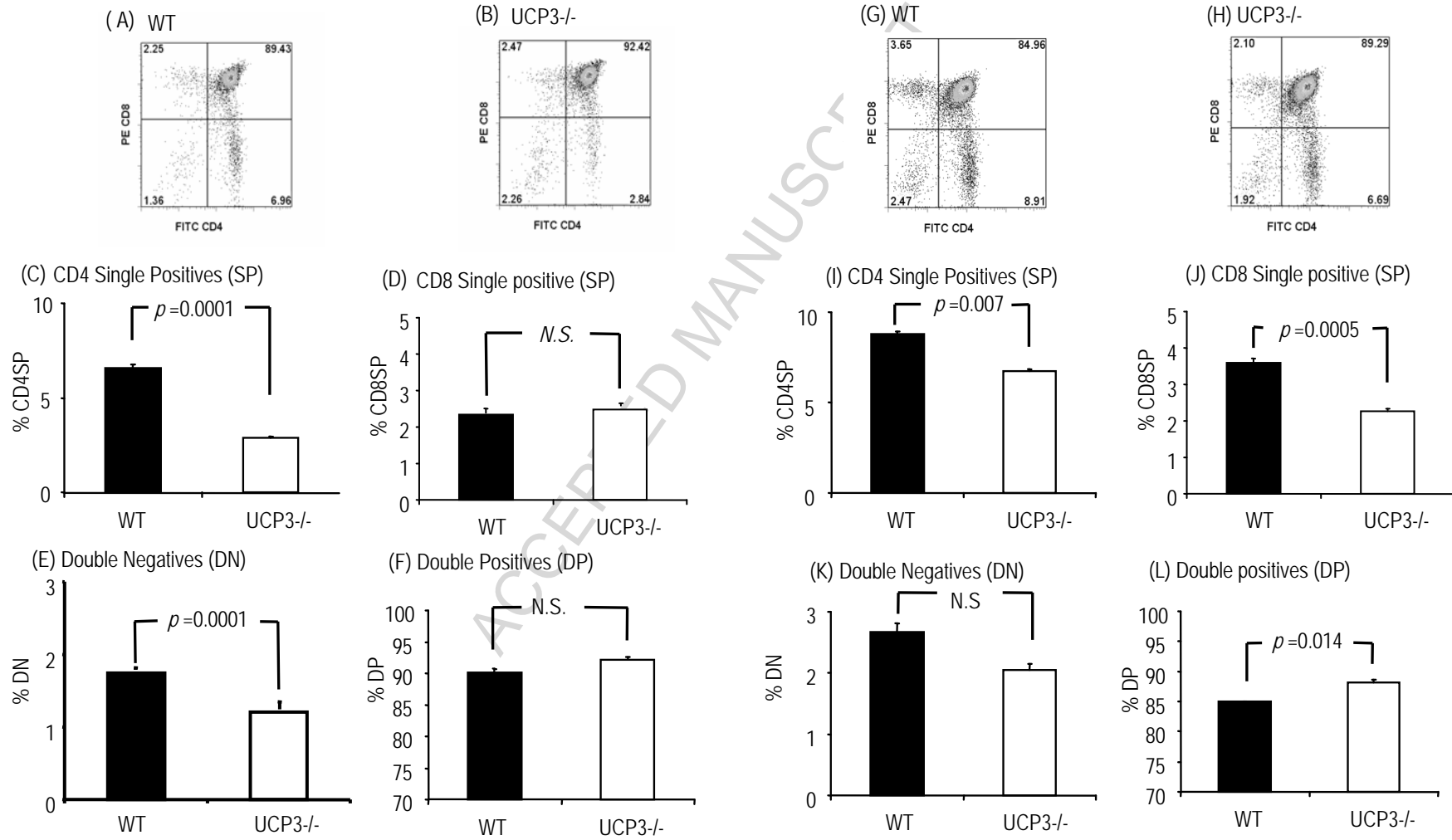


Figure 8

Spleen Cells: FED

Spleen Cells: FASTED

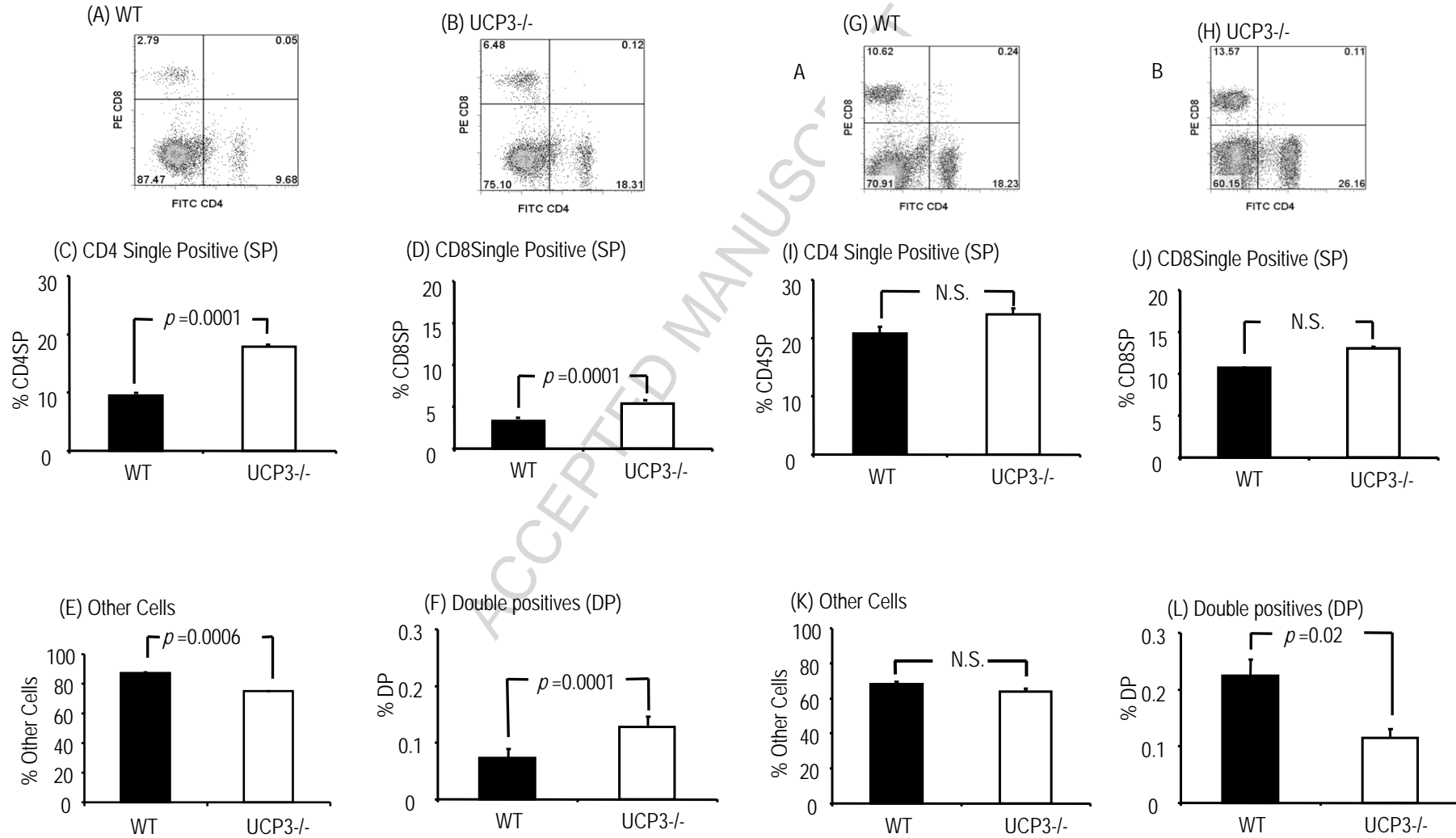


Figure 9

